



Satellite-transition double cross-polarization HETCOR under fast MAS

Ivan Hung, Zhehong Gan*

National High Magnetic Field Laboratory, 1800 East Paul Dirac Drive, Tallahassee, FL 32310, USA



ARTICLE INFO

Article history:

Received 13 December 2022

Revised 12 January 2023

Accepted 15 January 2023

Available online 20 January 2023

Keywords:

HETCOR

HMQC

Cross-polarization

Double cross polarization

Spinlock

Hartmann-Hahn

Quadrupolar nuclei

Satellite-transitions

Double quantum satellite-transition

Quadrupolar jolting frame

Average Hamiltonian

Effective field

Magic-angle spinning

Spinning sidebands

ABSTRACT

Double-cross polarization to the satellite-transitions (STs) of half-integer quadrupolar nuclei is demonstrated using proton-detected heteronuclear correlation (HETCOR) under fast magic-angle spinning (MAS). By placing the *rf* frequency away from the central-transition (CT) and selective to the STs, average Hamiltonian theory shows a scaled effective *rf* field with a phase equal to the complex ST spinning sideband being irradiated. Such an effective *rf* field can excite and spinlock STs but the phase spread usually leads to signal cancellation in one-step excitation or cross polarization experiments. The cancellation does not occur for two-step double cross-polarization (DCP) HETCOR experiments, therefore high efficiencies can be obtained. With careful magic-angle calibration, ST and double-quantum ST (DQST) HETCOR experiments are demonstrated with the ^{35}Cl nuclei in histidine-HCl-H₂O. These experiments provide additional information over the commonly observed CT spectra and near isotropic resolution in the case of DQST of spin $S = 3/2$ quadrupolar nuclei.

© 2023 Published by Elsevier Inc.

1. Introduction

Heteronuclear correlation (HETCOR) is a widely used experiment in solid-state NMR which provides through-bond and through-space information via scalar-*J* and dipolar (D) couplings. There are two categories of methods for establishing heteronuclear correlation. The first kind is based on the insensitive nuclei enhanced by polarization transfer (INEPT) [1] and heteronuclear multiple-quantum coherence (HMQC) [2] experiments originally developed for solution NMR spectroscopy. The second type uses cross-polarization (CP) with spinlock in the *rf* rotating frame first introduced for solid-state NMR spectroscopy [3]. The two categories use different parts of the heteronuclear coupling Hamiltonian, the *z* spin-operator terms for INEPT and HMQC vs the *x* and *y* terms for CP. Thus, the transfer processes are subject to different relaxation mechanisms (T_2 vs $T_{1\rho}$). For spins $S = 1/2$ like ^{13}C and ^{15}N in solids, the CP method is usually preferred given the fact that $T_{1\rho} \gg T_2$ in the presence of strongly coupled protons. Combined with magic-angle spinning (MAS), CPMAS [4] has become an ubiquitous

method for acquiring high-resolution spectra and HETCOR experiments for solids.

The situation becomes a bit more complex for spin $S > 1/2$ half-integer quadrupolar nuclei. As described in the seminal work by A. Vega [5,6], magic-angle spinning induces level crossings between the satellite-transitions (STs) and the spinlock *rf* frequency. These brief crossings can cause leakages of polarization, therefore strong *rf* fields should be avoided for the spinlock. Low *rf* fields are usually used to reduce the deteriorating effect of the spinlock to the central-transition (CT) polarization during CP. Low *rf* fields not only limit the bandwidth with respect to frequency offsets but also restrict the ^1H *rf* field that can be used to match the Hartmann-Hahn (HH) CP conditions [7] from being close to rotary resonances which interfere with the ^1H spinlock [8–11]. For these reasons, pulsed methods using INEPT and HMQC have been explored for indirect detection and HETCOR of quadrupolar nuclei [12–16]. The broad bandwidth obtained from using just two short pulses in HMQC offers opportunities for indirect detection of ST, multiple-quantum (MQ), and even overtone (OT) transitions of quadrupolar nuclei, including ^{14}N for which all single-quantum transitions are subject to large first-order quadrupolar broadening. In order to accelerate HMQC build-up, dipolar recoupling under

* Corresponding author.

E-mail address: gan@magnet.fsu.edu (Z. Gan).

MAS can be applied, namely D-HMQC, on the observed or indirect channel [14,17]. When applied on the observation channel, the dipolar recoupling also re-introduces the chemical shift anisotropy (CSA). Incomplete refocusing of the CSA due to spinning frequency fluctuations can cause t_1 -noise particularly for recoupling sequences that are sensitive to the rotor angle [18]. Improved pulse sequences such as TONE-HMQC [19], or by switching the recoupling to the indirect quadrupolar nuclei using the early-developed TRAPDOR [20,21], namely T-HMQC [22–24], have been developed to address the t_1 -noise issue. In general, various methods have their own pros and cons regarding bandwidth, efficiency, ^1H T_2 contributions to the indirect dimension, saturation and cancellation of large uncorrelated signals and other stability and robustness issues. The choices between the CP and various HMQC methods depend on the sample systems and experimental conditions such as the speed of MAS.

In this work, we explore cross-polarization to satellite-transitions of half-integer quadrupolar nuclei. Specifically, the two-step $^1\text{H} \rightarrow \text{X} \rightarrow ^1\text{H}$ or double CP (DCP), for ^1H -detected HETCOR experiments under fast MAS. In 2017, Carnevale *et al.* reported a highly efficient proton-detected $^1\text{H}/^{14}\text{N}$ experiment using DCP under MAS above 60 kHz [25]. It was a surprise observation considering that the amide ^{14}N has spinning sideband (ssb) manifolds that spread over several MHz. No one-step CP had previously been reported even for smaller quadrupolar couplings. This observation motivated subsequent studies on long rf pulses under large anisotropic interactions modulated by MAS. Using average Hamiltonian theory (AHT) in the quadrupolar jolting frame (QJF), the effective rf field can be derived and the result shows a scaling by the complex intensity of the spinning sideband near the rf frequency [23,24,26–28]. For individual crystallites, the phase of ^{14}N ssbs varies widely, therefore one-pulse excitation or one-step CP would lead to incoherent excitation (or CP) causing cancellation of the signals for powder samples. However, when a pair of long pulses are used as in the cases of HMQC and DCP HETCOR, the phase spread does not affect the encoding of the indirectly observed quadrupolar nuclei. Such is the key to why high efficiencies can be achieved for long-pulse HMQC and DCP HETCOR [23]. This idea has been extended to the design of novel satellite-transition magic-angle spinning (STMAS) [29] and multiple-quantum magic-angle spinning (MQMAS) [30,31] sequences using rotor period long ST pulses. These pulse sequences are highly efficient and require low rf power and have succeeded in obtaining isotropic spectra for the largest quadrupolar coupling to date.

In this work, we apply the mechanism described above to satellite-transitions of half-integer quadrupolar nuclei. HETCOR with satellite-transitions can provide additional information and opportunities over the more commonly recorded CT HETCOR spectra. These transitions have different peak positions and width due to their isotropic quadrupolar shift and second-order quadrupolar broadening remaining under MAS [32,33]. We will show that by interconverting between the single-quantum (SQ) and double-quantum (DQ) satellite-transitions using CT selective π -pulses, nearly isotropic resolution can be obtained for spin $S = 3/2$ nuclei [24]. It should be mentioned that all satellite-transition experiments require precise magic-angle setting to average out the large first-order quadrupolar interaction [34–36].

In the following, we first give a brief description of the theory. The effective Hamiltonian for ST-selective rf pulses in the quadrupolar jolting frame explains the mechanism by which DCP can be achieved more efficiently than one-step CP. Both one-step CP and DCP via CT or ST are compared experimentally using histidine-HCl-H₂O (**hist**) under 90 kHz MAS. The fast MAS has several advantages for satellite-transition CP HETCOR experiments. First, it improves the line width and lengthens T_2 as for all proton-detected

MAS experiments. Second, fast spinning leaves larger gaps among rotary resonance conditions $\omega_n^H = n\omega_1$ ($n = 1/2, 1, 2, \dots$) for the protons [8–11,37]. The large gaps help to reduce $T_{1\rho}$ contributions from the rotary resonance effect with the ^1H rf field used to match the HH CP conditions. Experimental optimizations and comparisons between $^1\text{H}/^{35}\text{Cl}$ single- and double-CP with the CT and ST will be presented. Near isotropic resolution from acquiring double-quantum ST HETCOR will be demonstrated for the spin $S = 3/2$ ^{35}Cl nucleus.

2. Theory

The derivation of the effective rf Hamiltonian in the presence of a large modulating quadrupolar interaction under MAS has been given in Refs. [23,24] for spin $S = 1$ and $3/2$. A summary of the first-order average rf Hamiltonian of a $S = 3/2$ spin is presented here for spinlock and CP. Higher order treatments and effective Hamiltonian by numerical calculations can also be found in Refs. [28,38,39] for the case of strong rf field. In the interaction representation or the jolting frame [26] of $H_Q(t) = q(t)[S_z^2 - S(S+1)/3]$ defined by a rotation operator $R = \exp[-i \int_0^t H_Q(t') dt']$, the rf Hamiltonian $\omega_1 S_x$ becomes

$$h_{rf}(t) = R(t)\omega_1(t)S_xR(t)^{-1} = \frac{\sqrt{3}\omega_1}{2} \begin{vmatrix} 0 & e^{i\varphi_Q(t)} & & \\ e^{i\varphi_Q(t)} & 0 & \blacksquare & \\ & \blacksquare & 0 & e^{-i\varphi_Q(t)} \\ & & e^{-i\varphi_Q(t)} & 0 \end{vmatrix} \quad (1)$$

Here $\varphi_Q(t) = 2 \int_0^t q(t') dt'$ is the rotation angle of the jolting frame which is also the signal phase accumulated by the modulating first-order quadrupolar frequency of the ST. Fourier expansion of the signal $\exp[i\varphi_Q(t)]$ gives the spinning sideband intensities s_k for the crystallite under MAS with angular frequency $\omega_r = 2\pi\nu_r$

$$e^{i\varphi_Q(t)} = \sum_k s_k e^{ik\omega_r t} \quad (2)$$

It is important to distinguish the sideband intensities of individual crystallites s_k and a rotor-averaged one s_k^2 . The individual sideband amplitude s_k is complex and its phase varies widely among the crystallites as a function of the rotor angle. The rotor-angle averaged sideband intensity equals to s_k^2 , which is smaller and absorptive [40–42]. The phase spread of s_k plays a key role for the effective rf field and the spin dynamics for pulses lasting at least one rotor-period long. The mean magnitude of the scaling factor s_k for the effective rf field can be estimated from the number of ssbs within the span of satellite-transition frequency $\sim 1.5\nu_Q$, of which ν_Q is the quadrupolar coupling frequency, and the normalization $\sum_k s_k^2 = 1$

$$\langle |s_k| \rangle \sqrt{\nu_r/1.5\nu_Q} < 1 \quad (3)$$

The CT elements in the rf Hamiltonian in Eq. (1) (denoted by black squares) can be neglected when the rf irradiation is applied far off-resonance from the CT. The ST-selective rf Hamiltonian becomes two separated blocks. We can also assume the ST irradiation near the n th spinning sideband without losing generality for the averaged rf Hamiltonian in the QJF

$$\bar{h}_{rf} = \pi\nu_1\sqrt{3} \begin{vmatrix} 0 & s_n & & \\ s_n^* & 0 & & \\ & & 0 & s_{-n} \\ & & s_{-n}^* & 0 \end{vmatrix} \quad (4)$$

This Hamiltonian can be expressed with the two-level spin $S = 1/2$ operators for the satellite-transitions $S_x^{ST}, S_y^{ST}, S_z^{ST}$

$$h_{rf}^{-ST} = \frac{\sqrt{3}}{2} |s_n| \omega_1 \exp(-i\varphi_n S_z^{ST}) S_x^{ST} \exp(i\varphi_n S_z^{ST}) \quad (5)$$

Here φ_n is the phase of the n th ST spinning sideband near the rf frequency. The rotation $\exp(-i\varphi_n S_z^{ST})$ implies a phase shift by φ_n to the effective field from the x direction. The $\frac{\sqrt{3}}{2}$ factor comes from the satellite-transition elements for the S_x operator of a spin $S = 3/2$. Eq (5) summarizes the effective rf Hamiltonian with a scaling factor $|s_n|$ and a phase shift φ_n .

3. Results and discussion

In the QJF, the large offset from the MAS-modulated quadrupolar coupling has been eliminated. Thus, ST polarization can be spinlocked by an on-resonance effective rf field at a direction defined by the phase φ_n of the complex ST spinning sideband s_n near the rf frequency. The nutation frequency about the effective rf , relevant to the CP, is scaled down by $|s_n|$. The spinlock enables CP from protons to the pair of two-level ST systems of $S = 3/2$ quadrupolar nuclei when the HH condition is matched with the scaled nutation frequency. The direction of the spinlock and the generated CP signal phase defined by φ_n varies widely. A powder average can lead to signal cancellation and low efficiency. The situation is different for $^1\text{H} \rightarrow \text{X} \rightarrow ^1\text{H}$ double-CP because the effective rf phase is the same between the two encoding pulses, and only the relative phase between the two pulses matters for the frequency encoding of the indirect dimension. Therefore, the phase spread does not lead to signal cancellation. This is the key mechanism behind efficient double-CP for HETCOR of quadrupolar nuclei.

Fig. 1 compares one-step $^{35}\text{Cl} \rightarrow ^1\text{H}$ CP from CT or STs and the double $^1\text{H} \rightarrow ^{35}\text{Cl} \rightarrow ^1\text{H}$ CP via CT or STs. We chose the reversed $^{35}\text{Cl} \rightarrow ^1\text{H}$ one-step CP so all four cases in Fig. 1 can be compared by detecting the ^1H signal of **hist**. Direct ^{35}Cl detection is not feasible for the small amount of sample in a 0.75 mm rotor. The results in Fig. 1 show the lowest signal from $^{35}\text{Cl}(\text{ST}) \rightarrow ^1\text{H}$ CP. It should be noted that the phase spread φ_n for the effective ST rf field is not completely random or evenly distributed as the powder average of s_n results in s_n^2 , which is smaller than $|s_n|$ but not zero. $^1\text{H} \rightarrow ^{35}\text{Cl}(\text{CT}) \rightarrow ^1\text{H}$ double-CP gives the highest signal with polarization originating from protons of approximately 10 times higher in gyromagnetic ratio over ^{35}Cl . The case of $^1\text{H} \rightarrow ^{35}\text{Cl}(\text{ST}) \rightarrow ^1\text{H}$ double CP is the second highest at $\sim 50\%$ compared to $^1\text{H} \rightarrow ^{35}\text{Cl}(\text{CT}) \rightarrow ^1\text{H}$. This is remarkable considering that the modulated ST frequencies span more than MHz, an order of magnitude larger than the rf field used. The high efficiency confirms experimentally the absence of signal phase cancellation as mentioned in the theory.

Average Hamiltonian theory in the QJF shows a scaled down effective rf Hamiltonian and ST nutation frequency $\omega_X = \frac{\sqrt{3}}{2} |s_n| \omega_1$ which is important in choosing an optimal CP condition under fast MAS for proton detected experiments. Under MAS, the HH CP conditions becomes $|\omega_X - \omega_H| = n\omega_r$ for the flip-flop zero-quantum CP (ZQCP) and $|\omega_X + \omega_H| = n\omega_r$ for flip-flip double-quantum CP (DQCP) [43]. Here ω_X and ω_H are the effective rf nutation frequencies for the two nuclei respectively. The primary conditions are $n = 1, 2$ due to the MAS modulation to the second-rank dipolar coupling that mediates the polarization transfer. Several factors need be considered in choosing the optimal CP condition. First, the spinlock nutation frequencies, ω_X and ω_H , should avoid the rotary resonance conditions $n\omega_r$ which can cause rapid polarization decay to the spinlock [8–11]. For protons, the rotary resonance includes $n = 1/2$ HORROR condition [10,11] from homonuclear dipolar cou-

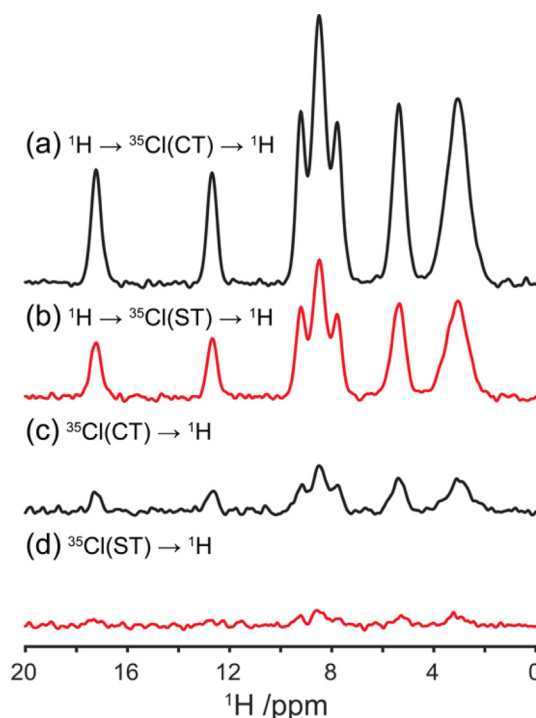


Fig. 1. Comparison of ^1H -detected (a) $^1\text{H} \rightarrow ^{35}\text{Cl}(\text{CT}) \rightarrow ^1\text{H}$, (b) $^1\text{H} \rightarrow ^{35}\text{Cl}(\text{ST}) \rightarrow ^1\text{H}$, (c) $^{35}\text{Cl}(\text{CT}) \rightarrow ^1\text{H}$, and (d) $^{35}\text{Cl}(\text{ST}) \rightarrow ^1\text{H}$ CP NMR spectra of **hist**. Experiments were carried out at $B_0 = 18.8$ T at the frequencies $\nu_0(^1\text{H}) = 800.12$ MHz and $\nu_0(^{35}\text{Cl}) = 78.40$ MHz using an 800 MHz Bruker Avance III HD spectrometer and a 0.75 mm MAS probe developed at the NRMFL. A spinning frequency of $\omega_r/2\pi = 90$ kHz was used, and for each CP transfer contact times of 17 ms, ^1H rf field amplitude ramp of 20 % centered at ~ 68 kHz, and ^{35}Cl rf fields $\gamma B_1/2\pi$ of ~ 12 and 26 kHz for the CT and ST spectra, respectively; 64 transients were averaged for each spectrum with recycle delays of 50 s for (a,b) and 8 s for (c,d). The transmitter offset was set near the ^{35}Cl CT for (a,c) and increased by +180 kHz near the second ST sideband for (b,d). A $\pi/2$ excitation pulse of 2 μs with ^1H rf field of 125 kHz was used for (a,b), and 4 μs pulse with ^{35}Cl rf field of 31.3 kHz for (c,d).

plings among protons in addition to the primary $n = 1, 2$ resonances [8,9]. Under slow MAS, $\omega_X, \omega_H \gg 2\omega_r$ avoid all rotary resonance conditions with practically achievable rf fields, and the $|\omega_X - \omega_H| = \omega_r$ ZQ CP condition is usually used. The ZQCP condition becomes practically difficult under fast MAS especially for quadrupolar nuclei as mentioned previously that strong rf fields cause polarization transfer and leakage among the various transitions within the $S > 1/2$ spin. Thus, the $|\omega_X + \omega_H| = \omega_r$ DQCP is often the optimal condition for CP. With the 90 kHz MAS used in this work, we chose $\omega_H \sim 0.75\omega_r$ between the $n = 1/2$ and 1 rotary resonance conditions for protons. High spinning frequencies widen the gap between these two resonance conditions to reduce their undesired $T_{1\rho}$ contributions to the spinlock. Faster MAS is advantageous in this regard for better ^1H spinlock under the DQCP condition.

The DQCP condition with $\omega_H \sim 0.75\omega_r$ requires $\omega_X = \frac{\sqrt{3}}{2} |s_n| \omega_1 \sim 0.25\omega_r$ for CP to the STs. The scaling factor $|s_n|$ varies among the crystallites in powder samples affecting the HH CP matching condition. A ramp of the ^1H rf field was applied to compensate the mismatch [44]. Fig. 2 shows the ^{35}Cl rf power calibration profiles for $^1\text{H} \rightarrow ^{35}\text{Cl} \rightarrow ^1\text{H}$ double CP via the CT and STs. The comparison clearly shows much higher rf power are necessary for the STs to make up for the scaling of the effective rf field. In addition, the matching profile is much broader than for the CT because of the distribution of the scaling factor $|s_n|$ for powder samples similar to the broadening of the CP matching profile from inhomogeneous rf fields. Ramping the ^1H rf field helps to compensate the mismatch, nevertheless the spread of the amplitude of the

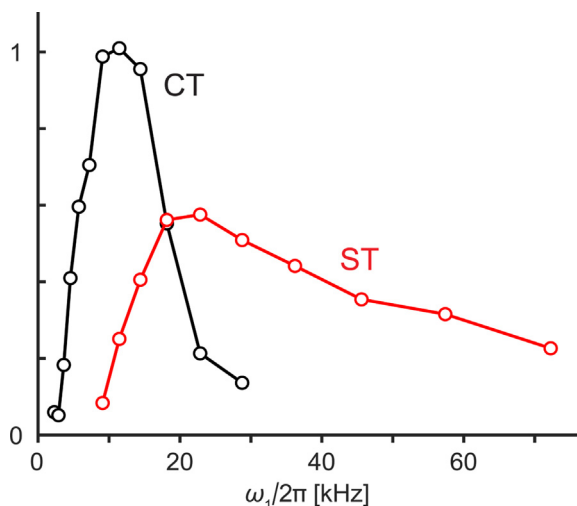


Fig. 2. Integrated ^1H intensity for the $^1\text{H} \rightarrow ^{35}\text{Cl}(\text{CT}) \rightarrow ^1\text{H}$ (black), and $^1\text{H} \rightarrow ^{35}\text{Cl}(\text{ST}) \rightarrow ^1\text{H}$ (red) double CP experiments as a function of the ^{35}Cl rf field amplitude $\gamma B_1/2\pi$ with a fixed ^1H $\omega_1 \sim 0.75\omega_r$. The transmitter offset was set near the ^{35}Cl CT for the black curve and increased by + 180 kHz for the ST red curve.

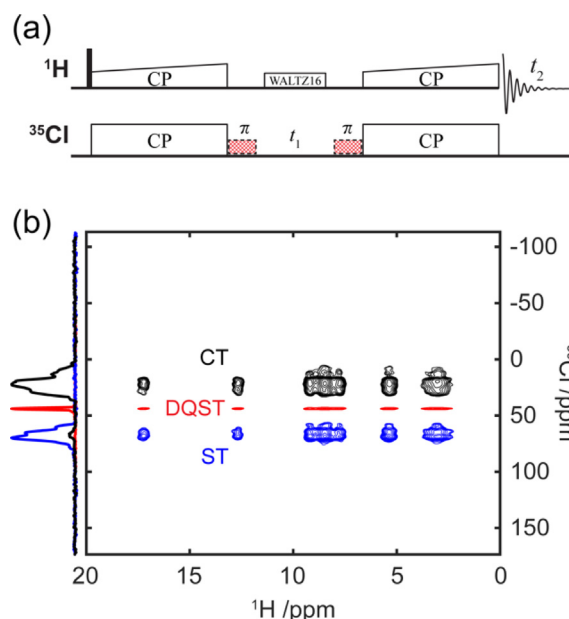


Fig. 3. (a) Pulse sequence schematic for the $^1\text{H} \rightarrow ^{35}\text{Cl}(\text{CT}, \text{ST}, \text{DQST}) \rightarrow ^1\text{H}$ double CP experiments. The two hashed CT-selective π -pulses are used to convert between SQ and DQ ST coherences and are omitted for CT and ST observation. (b) Overlay of two-dimensional ^1H -detected DCP NMR spectra of **hist** selecting the ^{35}Cl CT (black), ST (blue), or DQST (red) coherences with normalized projections. For the ST and DQST spectra, the transmitter offset was set + 180 kHz from CT near the second ST spinning sideband throughout, except for the CT-selective π -pulses. Each 2D experiment was acquired with indirect spectral widths of 22.5 kHz, 64 complex t_1 points, 16 transients per t_1 point, and a recycle delay of 10 s. Other experimental parameters are described in Fig. 1.

effective rf field still makes the CP less efficient, being the main cause to the $\sim 50\%$ ST signal compared with the CT signal in Fig. 1.

Fig. 3 shows an overlay of 2D $^1\text{H}/^{35}\text{Cl}$ HETCOR spectra of **hist** with the double CP conditions discussed above for the CT and STs. The magic-angle setting was carefully calibrated such that the large first-order quadrupolar coupling is averaged with rotor synchronized t_1 evolution [34] and only the isotropic and fourth-ranked second-order quadrupolar terms remain under MAS. For the spin $S = 3/2$ ^{35}Cl nuclei, the ratios of the isotropic and fourth-ranked terms between STs and CT are -2 and $-8/9$, respectively

[32,33]. By measuring the separation between STs and CT peaks, the chemical shift position can be determined from the -2 ratio for the isotropic quadrupolar shift between STs and CT. The spectra in Fig. 3 shows that the peaks from the STs and CT have similar width and are close to mirror images of each other as expected from the $-8/9$ ratio of their fourth-ranked terms. Acquisition of both CT and ST peaks allows for the separation of isotropic chemical and quadrupolar shift without the need of line shape fitting.

Single-quantum ST coherences can be converted to double-quantum ST (DQST) coherences with a CT selective π -pulse [45]. Fig. 3b shows a DQST HETCOR spectrum (red traces) by adding two CT π -pulses in the pulse sequence (Fig. 3a). The second order quadrupolar broadening to the DQSTs is $1/9$ in frequency or $1/18$ in ppm to that of CT. The ^{35}Cl dimension is nearly isotropic; made possible with double-CP to the STs. It is worth noting that TRAP-DOR recoupling can also generate correlation with all transitions including the DQSTs of a spin $S = 3/2$ simultaneously using the T-HMQC experiment [24]. Fig. 3 shows that near isotropic resolution can be obtained with both methods. In the present instance, the proton T_2 relaxation does not contribute to the ^{35}Cl linewidth as opposed to the case of T-HMQC. Spin-diffusion among protons can occur during the ^1H spinlock even under fast MAS causing relayed peaks in the DCP HETCOR spectra. The efficiency of the DCP is found to be about 2.7 times lower than optimized T-HMQC in Ref. [24], as measured by their first t_1 -increments. Besides the transfer efficiency, decay of the ^1H signal is a major factor contributing to the difference between a 1.7 ms spin-echo for the T-HMQC [24] and the 17 ms CP contact times used here for the DCP HETCOR.

4. Conclusions

It has been shown that double cross-polarization can be achieved efficiently with the satellite-transitions of half-integer quadrupolar nuclei using a selective ST spinlock. The offset from the large modulating first-order quadrupolar coupling has been treated in the quadrupolar jolting frame leading to a scaled effective rf field with the phase of the satellite-transition spinning sidebands near the rf frequency. The phase spread for the effective rf field usually causes signal cancellation for single-step excitation or CP but the cancellation does not occur for double CP. As a result, highly efficient HETCOR spectra can be obtained for the satellite-transitions as demonstrated for the ^{35}Cl nuclei in **hist** via protons under fast MAS. Satellite-transitions can provide additional information to the usually acquired central-transition spectra with careful magic-angle calibration. For spin $S = 3/2$ quadrupolar nuclei such as ^{35}Cl , the satellite-transition coherence can be converted efficiently to double-quantum satellite-transitions, which have nearly isotropic spectral resolution. Ultrafast MAS is important to these experiments not only for improved ^1H spectral resolution and sensitivity, but also for optimal double-quantum cross polarization to the satellite-transitions with minimal loss from rotary resonance effects to the spinlock.

Data availability

Data will be made available on request.

Declaration of Competing Interest

The authors declare that they have no known competing financial interests or personal relationships that could have appeared to influence the work reported in this paper.

Acknowledgements

This work was supported by the National High Magnetic Field Laboratory (NHMFL, USA) through NSF DMR-1644779 and the State of Florida.

References

- [1] G.A. Morris, R. Freeman, Enhancement of Nuclear Magnetic-Resonance Signals by Polarization Transfer, *J. Am. Chem. Soc.* 101 (1979) 760–762, <https://doi.org/10.1021/ja00497a058>.
- [2] L. Muller, Sensitivity Enhanced Detection of Weak Nuclei Using Heteronuclear Multiple Quantum Coherence, *J. Am. Chem. Soc.* 101 (1979) 4481–4484.
- [3] A. Pines, M.G. Gibby, J.S. Waugh, Proton-Enhanced NMR of Dilute Spins in Solids, *J. Chem. Phys.* 59 (1973) 569–590.
- [4] J. Schaefer, E.O. Stejskal, Carbon-13 nuclear magnetic resonance of polymers spinning at the magic angle, *J. Am. Chem. Soc.* 98 (1976) 1031–1032.
- [5] A.J. Vega, MAS NMR Spin Locking of Half-Integer Quadrupolar Nuclei, *J. Magn. Reson.* 96 (1992) 50–68, [https://doi.org/10.1016/0022-2364\(92\)90287-H](https://doi.org/10.1016/0022-2364(92)90287-H).
- [6] A.J. Vega, CP/MAS of quadrupolar S=3/2 nuclei, *Solid State Nucl. Magn. Reson.* 1 (1992) 17–32, [https://doi.org/10.1016/0926-2040\(92\)90006-U](https://doi.org/10.1016/0926-2040(92)90006-U).
- [7] S.R. Hartmann, E.L. Hahn, Nuclear Double Resonance in Rotating Frame, *Phys. Rev.* 128 (1962) 2042–2053.
- [8] T.G. Oas, R.G. Griffin, M.H. Levitt, Rotary Resonance Recoupling of Dipolar Interactions in Solid-State Nuclear Magnetic-Resonance Spectroscopy, *J. Chem. Phys.* 89 (1988) 692–695.
- [9] Z.H. Gan, D.M. Grant, Rotational Resonance in a Spin-Lock Field for Solid-State NMR, *Chem. Phys. Lett.* 168 (1990) 304–308.
- [10] N.C. Nielsen, H. Bildsoe, H.J. Jakobsen, M.H. Levitt, Double-Quantum Homonuclear Rotary Resonance - Efficient Dipolar Recovery in Magic-Angle-Spinning Nuclear-Magnetic-Resonance, *J. Chem. Phys.* 101 (1994) 1805–1812.
- [11] R. Verel, M. Baldus, M. Ernst, B.H. Meier, A homonuclear spin-pair filter for solid-state NMR based on adiabatic-passage techniques, *Chem. Phys. Lett.* 287 (1998) 421–428.
- [12] Z. Gan, Measuring amide nitrogen quadrupolar coupling by high-resolution N-14/C-13 NMR correlation under magic-angle spinning, *J. Am. Chem. Soc.* 128 (2006) 6040–6041.
- [13] S. Cavadini, A. Lupulescu, S. Antonijevic, G. Bodenhausen, Nitrogen-14 NMR spectroscopy using residual dipolar splittings in solids, *J. Am. Chem. Soc.* 128 (2006) 7706–7707.
- [14] Z.H. Gan, J.P. Amoureux, J. Trebosc, Proton-detected N-14 MAS NMR using homonuclear decoupled rotary resonance, *Chem. Phys. Lett.* 435 (2007) 163–169.
- [15] Y. Nishiyama, M. Malon, Z.H. Gan, Y. Endo, T. Nemoto, Proton-nitrogen-14 overent two-dimensional correlation NMR spectroscopy of solid-sample at very fast magic angle sample spinning, *J. Magn. Reson.* 230 (2013) 160–164.
- [16] D. Iuga, C. Morais, Z. Gan, D.R. Neuville, L. Cormier, D. Massiot, NMR Heteronuclear Correlation between Quadrupolar Nuclei in Solids, *J. Am. Chem. Soc.* 127 (2005) 11540–11541, <https://doi.org/10.1021/ja052452n>.
- [17] J. Trebosc, B. Hu, J.P. Amoureux, Z. Gan, Through-space R3-HETCOR experiments between spin-1/2 and half-integer quadrupolar nuclei in solid-state NMR, *J. Magn. Reson.* 186 (2007) 220–227, <https://doi.org/10.1016/j.jmr.2007.02.015>.
- [18] Z. Gan, 13C/14N heteronuclear multiple-quantum correlation with rotary resonance and REDOR dipolar recoupling, *Journal of Magnetic Resonance.* 184 (2007) 39–43, <https://doi.org/10.1016/j.jmr.2006.09.016>.
- [19] A. Venkatesh, X. Luan, F.A. Perras, I. Hung, W. Huang, A.J. Rossini, t1-Noise eliminated dipolar heteronuclear multiple-quantum coherence solid-state NMR spectroscopy, *Phys. Chem. Chem. Phys.* 22 (2020) 20815–20828, <https://doi.org/10.1039/d0cp03511d>.
- [20] C.P. Grey, W.S. Veeman, A.J. Vega, Rotational echo 14N/13C/1H triple resonance solid-state nuclear magnetic resonance: A probe of 13C–14N internuclear distances, *J. Chem. Phys.* 98 (1993) 7711–7724, <https://doi.org/10.1063/1.464579>.
- [21] C.P. Grey, A.J. Vega, Determination of the Quadrupole Coupling-Constant of the Invisible Aluminum Spins in Zeolite HY with 1H/27Al TRAPDOR NMR, *J. Am. Chem. Soc.* 117 (1995) 8232–8242, <https://doi.org/10.1021/ja00136a022>.
- [22] J.A. Jarvis, I.M. Haies, P.T.F. Williamson, M. Carravetta, An efficient NMR method for the characterisation of 14N sites through indirect 13C detection, *Phys. Chem. Chem. Phys.* 15 (2013) 7613, <https://doi.org/10.1039/c3cp50787d>.
- [23] I. Hung, P. Gor'kov, Z. Gan, Efficient and sideband-free 1H-detected 14N magic-angle spinning NMR, *J. Chem. Phys.* 151 (2019), <https://doi.org/10.1063/1.5126599>.
- [24] I. Hung, Z. Gan, High Resolution NMR of S = 3/2 Quadrupole Nuclei by Detection of Double-Quantum Satellite-Transitions via Protons, *J. Phys. Chem. Lett.* 11 (2020) 4734–4740, <https://doi.org/10.1021/acs.jpclett.0c01236>.
- [25] D. Carnevale, X. Ji, G. Bodenhausen, Double cross polarization for the indirect detection of nitrogen-14 nuclei in magic angle spinning NMR spectroscopy, *J. Chem. Phys.* 147 (2017), <https://doi.org/10.1063/1.5000689>.
- [26] P. Caravatti, G. Bodenhausen, R.R. Ernst, Selective pulse experiments in high-resolution solid state NMR, *J. Magn. Reson.* 55 (1983) 88–103, [https://doi.org/10.1016/0022-2364\(83\)90279-2](https://doi.org/10.1016/0022-2364(83)90279-2).
- [27] A.J. Pell, G. Kervern, L. Emsley, M. Deschamps, D. Massiot, P.J. Grandinetti, G. Pintacuda, Broadband inversion for MAS NMR with single-sideband-selective adiabatic pulses, *J. Chem. Phys.* 134 (2011), <https://doi.org/10.1063/1.3521491>.
- [28] A.J. Pell, K.J. Sanders, S. Wegner, G. Pintacuda, C.P. Grey, Low-power broadband solid-state MAS NMR of 14N, *J. Chem. Phys.* 146 (2017).
- [29] I. Hung, Z. Gan, Low-power STMAS - breaking through the limit of large quadrupolar interactions in high-resolution solid-state NMR spectroscopy, *Phys. Chem. Chem. Phys.* 22 (2020) 21119–21123, <https://doi.org/10.1039/d0cp04274a>.
- [30] I. Hung, Isotropic solid-state MQMAS NMR spectra for large quadrupolar interactions using satellite-transition selective inversion pulses and low rf fields, *J. Magn. Reson.* 324 (2021), <https://doi.org/10.1016/j.jmr.2021.106913>.
- [31] I. Hung, Z. Gan, On the use of single-frequency versus double-frequency satellite-transition pulses for MQMAS, *J. Magn. Reson.* 328 (2021), <https://doi.org/10.1016/j.jmr.2021.106994>.
- [32] J.P. Amoureux, C. Huguenard, F. Engelke, F. Taulelle, Unified representation of MQMAS and STMAS NMR of half-integer quadrupolar nuclei, *Chem. Phys. Lett.* 356 (2002) 497–504.
- [33] I. Hung, J. Trebosc, G.L. Hoatson, R.L. Vold, J.P. Amoureux, Z. Gan, Q-shear transformation for MQMAS and STMAS NMR spectra, *J. Magn. Reson.* 201 (2009) 81–86.
- [34] Z. Gan, Isotropic NMR spectra of half-integer quadrupolar nuclei using satellite transitions and magic-angle spinning, *J. Am. Chem. Soc.* 122 (2000) 3242–3243.
- [35] Z. Gan, Satellite transition magic-angle spinning nuclear magnetic resonance spectroscopy of half-integer quadrupolar nuclei, *J. Chem. Phys.* 114 (2001) 10845–10853.
- [36] C. Huguenard, F. Taulelle, B. Knott, Z. Gan, Optimizing STMAS, *J. Magn. Reson.* 156 (2002) 131–137, <https://doi.org/10.1006/jmre.2002.2548>.
- [37] I. Hung, Z. Gan, Spin-locking and cross-polarization under magic-angle spinning of uniformly labeled solids, *Journal of Magnetic Resonance.* 256 (2015) 23–29, <https://doi.org/10.1016/j.jmr.2015.04.005>.
- [38] S.V. Sajith, S. Jayanthi, A. Lupulescu, Effective Hamiltonian and 1H–14N cross polarization/double cross polarization at fast MAS, *J. Magn. Reson.* 320 (2020), <https://doi.org/10.1016/j.jmr.2020.106832>.
- [39] S.V. Sajith, S. Jayanthi, A. Lupulescu, Effective Hamiltonian and spin dynamics in fast MAS TRAPDOR-HMQC experiments involving spin-3/2 quadrupolar nuclei, *Solid State Nucl. Magn. Reson.* 122 (2022), <https://doi.org/10.1016/j.ssnmr.2022.101821>.
- [40] J. Herzfeld, A.E. Berger, Sideband Intensities in NMR-Spectra of Samples Spinning at the Magic Angle, *Journal of Chemical Physics.* 73 (1980) 6021–6030.
- [41] M.M. Maricq, J.S. Waugh, NMR in Rotating Solids, *Journal of Chemical Physics.* 70 (1979) 3300–3316.
- [42] M. Hohwy, H. Bildsoe, H.J. Jakobsen, N.C. Nielsen, Efficient Spectral Simulations in NMR of Rotating Solids. The γ -COMPUTE Algorithm, *J. Magn. Reson.* 136 (1999) 6–14, <https://doi.org/10.1006/jmre.1998.1593>.
- [43] B.H. Meier, Cross Polarization under Fast Magic Angle Spinning - Thermodynamical Considerations, *Chem. Phys. Lett.* 188 (1992) 201–207.
- [44] G. Metz, X.L. Wu, S.O. Smith, Ramped-Amplitude Cross-Polarization in Magic-Angle-Spinning NMR, *J. Magn. Reson. A.* 110 (1994) 219–227.
- [45] H.T. Kwak, Z.H. Gan, Double-quantum filtered STMAS, *J. Magn. Reson.* 164 (2003) 369–372.